



Prediction of subcutaneous drug absorption – Development of novel simulated interstitial fluid media for predictive subcutaneous *in vitro* assays

Iria Torres-Terán^{a,b}, Márta Venczel^a, Sandra Klein^{b,*}

^a University of Greifswald, Department of Pharmacy, Institute of Biopharmaceutics and Pharmaceutical Technology, Center of Drug Absorption and Transport, 3 Felix Hausdorff Street, 17489 Greifswald, Germany

^b Sanofi-Aventis Deutschland GmbH, R&D, Global CMC Development, Synthetics Platform, Industriepark Hoechst, H770, D-65926 Frankfurt am Main, Germany

ABSTRACT

Media that mimic physiological fluids at the site of administration have proven to be valuable *in vitro* tools for predicting *in vivo* drug release, particularly for routes of administration where animal studies cannot accurately predict human performance. The objective of the present study was to develop simulated interstitial fluids (SISFs) that mimic the major components and physicochemical properties of subcutaneous interstitial fluids (ISFs) from preclinical species and humans, but that can be easily prepared in the laboratory and used in *in vitro* experiments to estimate *in vivo* drug release and absorption of subcutaneously administered formulations. Based on data from a previous characterization study of ISFs from different species, two media were developed: a simulated mouse-rat ISF and a simulated human-monkey ISF. The novel SISFs were used in initial *in vitro* diffusion studies with a commercial injectable preparation of liraglutide. Although the *in vitro* model used for this purpose still requires significant refinement, these two new media will undoubtedly contribute to a better understanding of the *in vivo* performance of subcutaneous injectables in different species and will help to reduce the number of unnecessary *in vivo* experiments in preclinical species by implementation in predictive *in vitro* models.

1. Introduction

Subcutaneous (SC) administration is an important secondary route of drug delivery, accounting for 20 % of the drugs approved by the European Medicines Agency (Dubbelboer and Sjögren, 2022). More than five-sixths of the drugs approved for SC administration are biologics, the rest are small molecules (Dubbelboer and Sjögren, 2022). The SC route is used to achieve a systemic effect after injecting the drug product into the interstitial space of the SC tissue, also known as the hypodermis. This tissue, composed mainly of loose connective and adipose tissue, is perfused by an ultrafiltrate of plasma, the interstitial fluid (ISF) (Viola et al., 2018). Since the ISF interacts with the formulation after injection, its composition and properties are essential for understanding drug absorption after subcutaneous administration. Moreover, it would be important to be able to reproduce this fluid when establishing *in vitro* models aimed at predicting the *in vivo* performance of subcutaneously administered drugs. Although *in vitro* tests have traditionally been used for quality control, they are increasingly used in the early stages of development in many areas of drug development to estimate the *in vivo* performance of new drug candidates and formulations (Collins et al., 2020; Sánchez-Félix et al., 2020). With regard to *in vivo* performance,

meaningful *in vitro* tests would be particularly important for the SC pathway, as animal studies provide poor predictions of human *in vivo* performance (Sánchez-Félix et al., 2020; Viola et al., 2018; Zheng et al., 2012). By mimicking the composition and essential properties of ISF, a better representation of the SC environment in *in vitro* assays could be achieved, which would likely improve the predictive power of such assays (Torres-Terán et al., 2021). To date, however, there is still a lack of appropriate biorelevant and/or physiologically relevant *in vitro* media. Characterization of the composition and physicochemical properties of ISF could facilitate the development of media that mimic ISF characteristics relevant to SC drug release and absorption. (Collins et al., 2020; D'Arcy et al., 2022; Sánchez-Félix et al., 2020; Torres-Terán et al., 2021).

For a long time, there have been no real efforts to develop so-called biorelevant *in vitro* models to predict the *in vivo* performance of subcutaneously administered preparations such as hormones, peptides or small molecules. *In vitro* release methods described so far are either based on the use of apparatus and media originally developed for other dosage forms (Del Curto et al., 2003; Gao et al., 2021, 2020) or are customized experimental setups of rather simple design, such as incubator shaker-based methods (Sun et al., 2002). Typically, drug release is

* Corresponding author at: University of Greifswald, Department of Pharmacy, Institute of Biopharmaceutics and Pharmaceutical Technology, Center of Drug Absorption and Transport, Felix-Hausdorff-Strasse 3, 17489 Greifswald, Germany.

E-mail address: sandra.klein@uni-greifswald.de (S. Klein).

<https://doi.org/10.1016/j.ijpharm.2024.124227>

Received 8 April 2024; Received in revised form 10 May 2024; Accepted 11 May 2024

Available online 13 May 2024

0378-5173/© 2024 The Author(s). Published by Elsevier B.V. This is an open access article under the CC BY-NC-ND license (<http://creativecommons.org/licenses/by-nc-nd/4.0/>).

determined using the “sample and separate” method (Cai et al., 2012; Chu et al., 2006; Negrín et al., 2004; Solano et al., 2013; Xuan et al., 2013), but in the customized setups dialysis methods are also common (D’Souza et al., 2014; Gao et al., 2007; Nippe et al., 2013). Typical media used in the *in vitro* release experiments comprise simple buffers such as phosphate buffer (D’Souza et al., 2014; Negrín et al., 2004; Nippe et al., 2013; Sun et al., 2002; Vlugt-Wensink et al., 2007), phosphate-buffered saline (PBS) (Cai et al., 2012; Chu et al., 2006; Doty et al., 2017; Gao et al., 2007; Lee et al., 2020; Li et al., 2015; Solano et al., 2013; Sun et al., 2008), and Hanks buffer (Iyer et al., 2007), i.e., media whose composition is not derived from ISF. Although the use of such *in vitro* release methods has in some cases shown a correlation between *in vitro* drug release and *in vivo* absorption (Gao et al., 2020, 2021), this does not necessarily imply that the respective method will be equally predictive for other drug formulations (Torres-Terán et al., 2021).

First attempts to develop predictive *in vitro* assays for SC injectables have recently been made using small molecules (Lou and Hageman, 2023), insulins (Bock et al., 2020), and monoclonal antibodies (Kinnunen et al., 2015) as model compounds. Kinnunen et al. described a dialysis-based system which aimed to simulate the SC environment using an artificial extracellular matrix embedded in a bicarbonate-based physiological buffer also referred to as the Subcutaneous Injection Site Simulator (SCISSOR) (Kinnunen et al., 2015). Bender et al. recently assessed the predictivity of a versatile set of *in vitro* tools that intended to mimic SC tissue properties, including apart from the SCISSOR, artificial matrices containing components of the SC tissue (e.g. collagen and hyaluronic acid) and dialysis membranes as well as different dissolution apparatuses; particularly USP apparatus 4 (Flow-Through Cell) and a small-volume version of USP apparatus 7 (Reciprocating Holder) (Bender et al., 2022). *In vitro* release of eight model compounds, including insulins, monoclonal antibodies, a cytokine, and an antigen-binding fragment was studied in either compendial media, e.g. PBS or artificial buffers used for mimicking ISF, such as the bicarbonate-based physiological buffer described by Kinnunen et al. (Kinnunen et al., 2015), and AQLX®, a non-phosphate buffer originally designed for preservation of tissues or cells during transport (Rees, 2011a). *In vitro* release data of the aforementioned compounds were compared with published human pharmacokinetic data such as AUC, C_{max} and t_{max} and the Pearson correlation coefficient was employed to assess the predictive power of the *in vitro* assays studied. The results of this calculation indicated that the *in vitro* models used in this study have limited predictive power in terms of predicting the *in vivo* performance of the tested formulations after SC administration in humans (Bender et al., 2022).

Recently, there has been an increase in activities related to the evaluation and/or development of *in vitro* tools (Bock et al., 2020; Kinnunen et al., 2015; Lou and Hageman, 2023) and media (Gao et al., 2020; Kinnunen et al., 2015; Rees, 2011b) for SC administered formulations. The media in particular have attracted increasing interest. Efforts have been made to develop the first biorelevant media for *in vitro* release studies of SC formulations, but it must be noted that the media proposed so far for *in vitro* testing of SC formulations have been developed solely on the basis of literature data derived from experiments that were not specifically conducted for this purpose (Torres-Terán et al., 2021). Due in particular to the difficulty in obtaining sufficient quantities of liquid for comprehensive analysis, data on the composition and properties of ISF are only available to a limited extent and the data sources for the media developed to date are very heterogeneous. It should also be noted that the data used are influenced by the method used to isolate the ISF and are therefore subject to errors, which is why they should be used with caution (Torres-Terán et al., 2021). In contrast, biorelevant media, especially those that have been successfully used to estimate the *in vivo* release of orally administered drugs, have been developed based on in-depth characterization studies of the relevant physiological fluids at the site of release in the context of dedicated experiments (Klein, 2010). Reliable *in vivo* data are the cornerstone for

the development of biorelevant media. In a previous study, ISF was isolated from SC tissues of five preclinical species, i.e. mice, rats, minipigs, landrace pigs, non-human primates, and humans, and characterized with respect to its major components and physicochemical properties. The data provided fundamental information for the development of biorelevant ISF media for both preclinical species, in particular rodents (mice/rats), monkeys and humans (Torres-Terán et al., 2023). The aim of the present work was to utilize these data to develop biorelevant ISF media that can subsequently be incorporated into biorelevant *in vitro* models to predict the *in vivo* performance of subcutaneously administered formulations.

2. Materials

Sodium chloride, sodium phosphate (dibasic and monobasic) and hyaluronic acid sodium salt were purchased from Fisher Scientific GmbH, Schwerte, Germany) while potassium chloride and magnesium chloride hexahydrate were acquired from Sigma Aldrich (Sigma Aldrich Chemie GmbH, Steinheim, Germany). Water of HPLC grade was produced using a MilliQ system (Merck KGaA, Darmstadt, Germany). FibrinCol®, Bromocresol Green Albumin assay kit (MAK124) and Bovine Serum Albumin were acquired from Sigma-Aldrich (Sigma Aldrich Chemie GmbH, Steinheim, Germany). ThinCert® Transwell plates were purchased from Greiner Bio-One GmbH (Frickenhausen, Germany). 3 mL liraglutide (6 mg/mL) prefilled pens (Victoza®, Novo Nordisk A/S, Bagsværd, Denmark, batch number: MP5A324) were obtained by prescription via a local Pharmacy.

3. Methods

3.1. Simulated interstitial fluid development

The simulated ISF media (SISFs) were developed with the aim of replicating as closely as possible the experimental data obtained for preclinical species and humans in the previous study (Torres-Terán et al., 2023), but keeping the overall composition and preparation of the media simple so that their use would be easy to implement in a biopharmaceutical laboratory. The target parameters were pH, osmolality, electrolyte, and albumin content, whereby the mean values of the corresponding experimental data were used in each case (Torres-Terán et al., 2023), while buffer capacity, colloid osmotic pressure and surface tension were assessed after preparation and compared with the reference data available for the target species groups.

Since very similar results for pH, osmolality and electrolyte content were obtained for the ISF of the preclinical animal species and humans, the same target values for these parameters were selected for the ISFs to be established. Accordingly, 138.5 mM sodium (Na^+), 10.0 mM potassium (K^+), 1.8 mM calcium (Ca^{2+}), 0.8 mM magnesium (Mg^{2+}), 4.2 mM phosphate (PO_4^{3-}) (representative of the experimentally determined phosphorus content), and 113.2 mM of chloride (Cl^-) were set as target values for the electrolyte composition (Torres-Terán et al., 2023). First, a buffer with good buffering properties at physiological pH (pH 7.4) was prepared from dibasic and monobasic sodium phosphate according to the target concentrations, and then the remaining electrolytes were added, taking care not to exceed the target osmolality (Table 1). The resulting buffer was defined as Blank SISF.

For the albumin content, there were clear differences between some species, especially non-human primates and the other preclinical species, while the data from non-human primates and humans were very similar. Since only one data set from a single animal was available for minipigs and landrace pigs, these species were not considered in the further course of the study. Accordingly, the data obtained from mice and rats were used to calculate the target parameters for the albumin content for the subgroup of preclinical species, while the corresponding data from non-human primates were summarized with those of humans. This resulted in two media (Fig. 1): the simulated mouse-rat ISF (SMR-

Table 1

Target (A) and reference (B) parameters for the simulated mouse-rat- (SMR) and human-monkey (SHM) ISFs (* plasma data were set as maximum).

(A)	Mouse-Rat	Human-Monkey
Na ⁺ (mM)	138.5	138.5
K ⁺ (mM)	10.0	10.0
Ca ²⁺ (mM)	1.8	1.8
Mg ²⁺ (mM)	0.8	0.8
Total phosphate (mM)	4.2	4.2
Cl ⁻ (mM)	113.2	113.2
Albumin (g/L)	17.5	30.0
pH	7.4	7.4
Osmolality (mOsm/kg)	295–300	295–300

(B)	Mouse-Rat	Human-Monkey
Buffer Capacity (μmol/(mL*ΔpH))	≤11.9 ± 0.5*	≤14.1 ± 0.5*
Colloid Osmotic Pressure (mmHg)	9 ± 0	16 ± 3.7
Surface Tension (mN/m)	51.5 ± 0.2	46.5 ± 0.2

ISF) and the simulated human-monkey ISF (SHM-ISF). Bovine serum albumin was chosen for the simulation of albumin due to its accessibility and affordability, in order to keep media production as streamlined as possible and to use the same excipients for both media. The target and reference parameters for the simulated media to be developed can be found in Table 1. In the event that the target parameters did not meet the desired physicochemical properties, slight adjustments were made in the electrolyte composition of the media. 0.05 % sodium azide was added to the final media to prevent the growth of microorganisms.

In the particular case of buffer capacity, for which there are no valid data in the literature and which could not be measured in the previous characterization study, the buffer capacity of the plasma samples

examined in the previous study was taken as the upper limit for the reference value (Torres-Terán et al., 2023). Specifically, the buffer capacity of rat plasma was chosen for the SMR-ISF design and the buffer capacity of human plasma for the SHM-ISF design.

3.2. Preparation of the simulated interstitial fluids

The following protocol was established for the preparation of 1 L of medium at a time:

- about 0.8 L of purified water is placed in a volumetric flask, a magnetic stirring bar is added, and the flask is placed on a magnetic stirring plate
- to achieve the target anion and cation concentrations listed in Table 1, a mixture of sodium-, potassium-, magnesium- and calcium chloride and (di) sodium (hydrogen) phosphate (the exact quantitative composition of which was to be determined in the course of the study) is added to the volumetric flask and dissolved while stirring
- the required amount of albumin is weighed and added in portions under gentle stirring (100 rpm)
- once all the albumin has been added, the mixture is stirred for a further 30-60 min at 100 rpm
- after complete dissolution of the electrolytes and dispersion of albumin, 0.05 % (w/v) sodium azide is added and the mixture is stirred further until its dissolution
- the pH value of the medium is checked and adjusted to 7.4 if necessary
- after removing the magnetic stirrer, the volume is filled up to 1.0 L with purified water and the contents of the flask are homogenized by gentle shaking

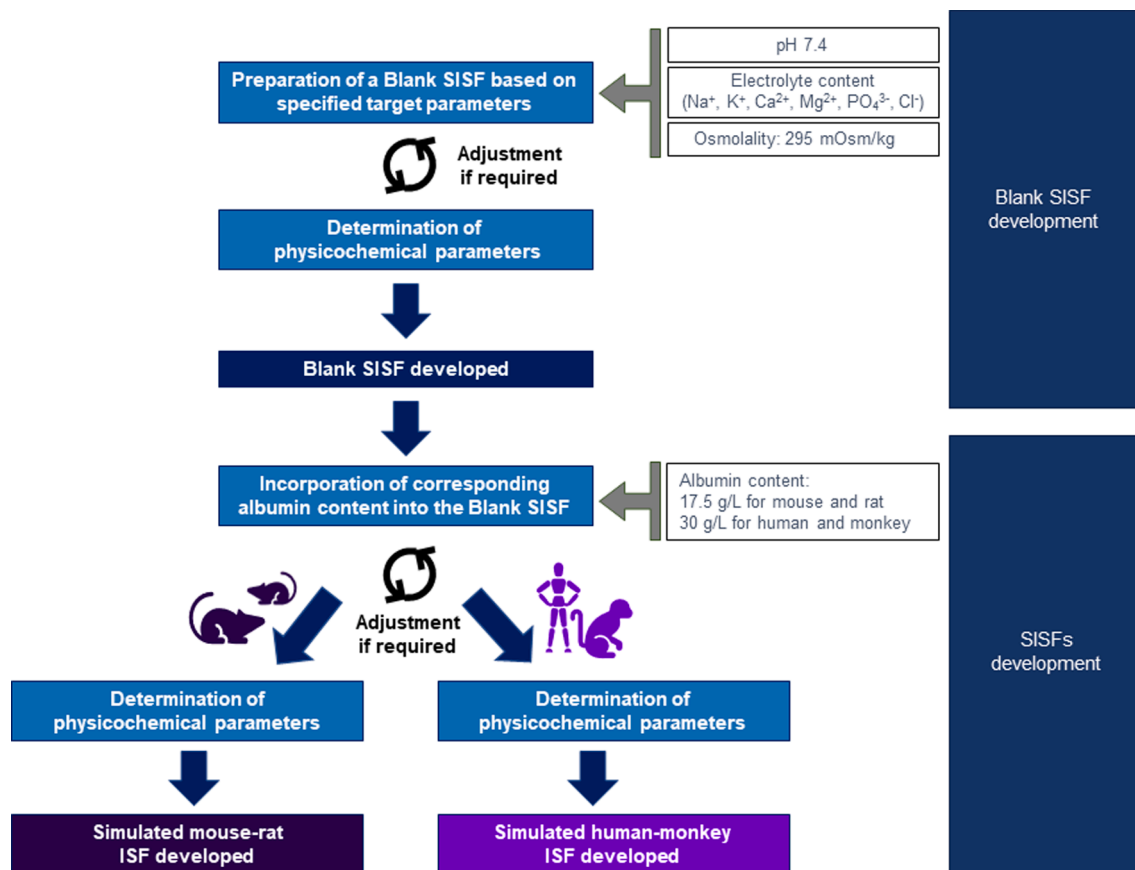


Fig. 1. Schematic representation of the development of Blank Simulated Interstitial Fluid (SISF) and Simulated Interstitial Fluids (SISFs) for different species.

3.3. Physicochemical characterization of the simulated interstitial fluids

Unless otherwise stated, all physicochemical determinations were performed in triplicate (n = 3).

3.3.1. pH

A calibrated pH-meter (WTW inoLab 7310P, Xylem Analytics Germany Sales GmbH & Co. KG, Mainz, Germany) was utilized for the pH determination of the media at 34 °C.

3.3.2. Buffer capacity

For the determination of the buffer capacity, the media were titrated with HCl (0.1 M) at 34 °C until a pH change of one unit occurred. The utilized quantity of the acid was measured for calculating the buffer capacity, based on the following equation " $\beta = \Delta\text{HCl}/\Delta\text{pH}$ "; where ΔHCl is the quantity of HCl added in mols, and ΔpH is the pH change of the media, induced by HCl.

3.3.3. Colloid osmotic pressure

The colloid osmotic pressure was determined with an Osmomat 050 (Gonotec GmbH, Berlin, Germany), which consists of a measuring cell composed of two compartments separated by a semipermeable membrane with 20 kDa pore size (Gonotec GmbH, Berlin, Germany). The upper compartment was filled with 500 μL of the media, and the lower compartment, with Ringer solution (B. Braun Melsungen AG, Melsungen, Germany), as recommended by the manufacturer. The differences in osmotic pressure generated by the two liquids lead to the permeation of solvent from the lower to the upper compartment until equilibrium is reached. This creates a negative pressure in the lower compartment, which is converted into an electrical signal that is linked to the colloid osmotic pressure of the analyzed medium.

3.3.4. Osmolality

The osmolality of the media was measured by determining the freezing point depression with the Osmomat 010 (Gonotec GmbH, Berlin, Germany), which was previously calibrated with a 400 mOsm/kg standard solution.

3.3.5. Surface tension

The surface tension of the media was determined at room temperature (20.5 ± 1.0 °C), via the pendant drop method, with an optical tensiometer (Theta Flex, Attension, Biolin Scientific, Stockholm, Sweden), which had previously been calibrated with MilliQ water at room temperature.

3.4. Stability assessment

The physical stability of the SISFs was assessed under two conditions: testing and storage. To assess media stability under testing conditions, buffers were placed in an incubator hood (TH 30, Edmund Bühler GmbH, Bodelshausen, Germany) at 34 °C and shaken at a low speed (70 rpm). To test the media stability under storage conditions, buffers were kept in a refrigerator (5 °C). In both cases, the stability study was run for 8 days and samples were taken at days 0, 1, 3 and 8. The pH, buffer capacity, osmolality and surface tension of the samples were evaluated in triplicates as described in Section 3.3. In addition, the media were visually inspected to ensure that no changes had occurred during the study period.

3.5. In vitro diffusion experiments

The first *in vitro* experiments performed with newly developed media were aimed at analyzing the influence of the composition of SISFs on the diffusion of the model drug liraglutide from the interstitial space into the plasma. To this end, a series of *in vitro* diffusion experiments were performed using a modified version of the artificial subcutaneous tissue

(AST) assay (Fig. 2) described by Schöner *et al.* (Schöner *et al.*, 2024). Liraglutide was selected due to its high albumin binding (>95 %) (Summary of Product Characteristics: Liraglutide[®], 2022) in particular to investigate the influence of the protein content of ISF of different species on the mobility of the drug. The basic experimental setup consisted of a ThinCert[®] Transwell plate with an insert of a polyethylene terephthalate membrane (0.4 μm pore size and 1×10^8 cm^2 pore density) and a hydrogel matrix layer developed by Schöner *et al.* The latter contained 0.1 % hyaluronic acid, 2 mg/mL collagen I, 15 μM serum albumin and 20 mM phosphate-buffered saline (PBS). In contrast to the matrix used in the experiments of Schöner *et al.*, bovine serum albumin was used in the present study instead of human serum albumin.

The simulated extracellular matrix was prepared as follows: 400 μL of a 1 % hyaluronic acid solution in 1x PBS, 0.08 mL of a 0.1 M NaOH solution, 0.72 mL of 5x PBS, 1 mL H₂O and 1 mL of a 60 μM serum albumin solution were added to the same vial and mixed intensively. The resulting solution was then pipetted into a second tube containing 800 mg of a 10 mg/L FibrilCol[®] solution and the resulting mixture was gently shaken to produce the initially liquid hyaluronic acid-collagen matrix. Of this, 250 μL mL was pipetted onto the apical side of the inserts of each Transwell plate and incubated at 37 °C for 1 h. At the end of this incubation period, 1.5 mL of 20 mM phosphate buffer was added to the basolateral compartment and the Transwell plate was stored overnight at 4 °C. As described by Schöner *et al.*, this conditioning ensured the desired consistency of the matrix (Schöner *et al.*, 2024).

The next day, the buffer from the basolateral (acceptor) compartment was replaced with 1.5 mL of simulated plasma (SPlasma) and the Transwell plate was incubated at 34 °C, 300 rpm for 1 h in an Eppendorf ThermoMixer C (Eppendorf SE, Hamburg, Germany). After incubation, the apical (donor) compartment was first filled with 100 μL SISF, into which 50 μL Liraglutide injection solution was then pipetted. The Transwell plate was then shaken for 8 h at 34 °C and 300 rpm. During this period, 50 μL samples were taken from the basolateral compartment at predetermined time points and analyzed by HPLC. After each sample removal, 50 μL of fresh medium were pipetted into the acceptor compartment.

As the development of SPlasma was not the subject of this study, as a first step, phosphate-buffered saline (PBS) was used to simulate essential physicochemical properties of plasma. PBS, which has a similar pH and osmolality to plasma, has already been used frequently in the past as a plasma surrogate for dissolution studies (D'Arcy *et al.*, 2022) either as a simple buffer (Rawat *et al.*, 2012) or in combination with albumin (Díaz de León-Ortega *et al.*, 2021), fetal bovine serum (Jablonka *et al.*, 2019) or cyclodextrins (Jablonka *et al.*, 2019; Wallenwein *et al.*, 2019). However, it should be noted that only a few studies aimed to simulate the physiological protein concentration of plasma (D'Arcy *et al.*, 2022; Díaz de León-Ortega *et al.*, 2021). As one of the aims of the study was to evaluate the impact of typical serum albumin concentrations on drug diffusion and thereby to increase the biorelevance of the *in vitro* model used, PBS was spiked in a second step with albumin concentrations determined in the previous characterization study for the respective species (25 g/L for SMR-Plasma and 60 g/L for SHM-Plasma).

In a second set of experiments, the AST assay was further modified to better understand how much the SISF composition as such would affect diffusion and to investigate the influence that the matrix might have on the diffusion of liraglutide. For this purpose, the experimental procedure was modified in such a way that the use of the extracellular matrix was omitted, but all other experimental details remained unchanged.

3.5.1. Drug quantification

All samples were analyzed with an Agilent 1260 high-performance liquid chromatograph (HPLC). (Agilent Technologies Deutschland GmbH, Waldbronn, Germany). 10 μL samples were injected with a G1329B Agilent autosampler, onto a Jupiter C18 Phenomenex column (5 μm , 2.1 x 150 mm) (Phenomenex Ltd., Aschaffenburg, Germany) maintained at 50 °C and analyzed with a G1321B fluorescence detector

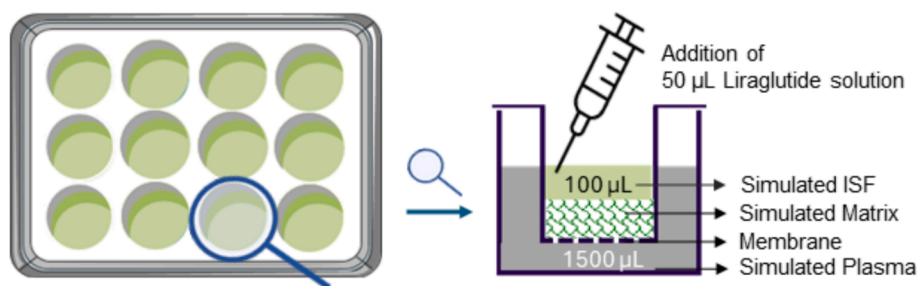


Fig. 2. Schematic representation of the Transwell-plate setup utilized for the artificial subcutaneous assay and one of the twelve wells in which the four main components (simulated ISF, simulated matrix, membrane, and simulated plasma) can be seen (adapted from Schönert et al., 2024).

(excitation at 285 nm and emission at 350 nm). The run time was 30 min and a gradient method with a constant flow rate of 1.0 mL/min was applied (Table 2). The composition of the two mobile phases was 89.75 % H₂O, 10 % ACN, 0.25 % TFA for the mobile phase A, and 89.75 % ACN, 10 % H₂O and 0.25 % TFA for the mobile phase B. Linearity of the method was screened for concentration ranges of 4.6 to 150 µg/mL before each run and in all cases the R² was above 0.996. The determined LOQ was 0.5075 µg/mL.

4. Results and discussion

4.1. Development of the simulated interstitial fluids

In the first step of the Blank SISF development, the ion composition and total electrolyte concentration of the medium were adjusted to the values listed in section 3.1, which originate from the previously published characterization study (Torres-Terán et al., 2023). For the resulting Blank SISF, this resulted in a buffer capacity of 4.8 µmol/(mL*ΔpH), which was two to three times lower than the reference values. However, as this parameter can have a significant impact on drug dissolution/release, the buffer capacity of the medium to be established should be as close as possible to the physiological reference value, which is why a compromise was made in this case. Accordingly, the phosphate content of the medium was increased from 4.2 to 19.8 mM to achieve a higher buffer capacity of around 10.5 µmol/(mL*ΔpH), as shown in Table 3. Moreover, during the development of the medium, it became clear that the addition of the target concentration of Ca²⁺ (1.8 mM) to the medium resulted in precipitation of CaHPO₄. Hence, Ca²⁺ was excluded from the medium. The final compositions of SMR-ISF and SHM-ISF were obtained by adding 17.5 g/L and 30 g/L albumin, respectively, to Blank SISF (Table 3). This resulted in a slight increase in buffer capacity. As mentioned above, the buffer capacity of plasma was set as the upper limit for the simulated ISFs to ensure that, although it could not be determined in the previous *ex vivo* experiments, it was not outside the estimated physiological range. The addition of albumin also led to the desired change in other media properties. For example, the amount of albumin added directly influenced the osmolality, which increased in each case and was within the physiological range with mean values of 281 and 290 mOsm/kg for SMR-ISF and SHM-ISF respectively (Torres-Terán et al., 2021). Similarly, compared to blank

Table 2
HPLC gradient of eluents A and B utilized for the liraglutide analysis.

Time (min)	Flow (mL/min)	A (%)	B (%)
0.0	1.0	95	5
0.2	1.0	95	5
2.0	1.0	74	26
9.7	1.0	64	36
14.8	1.0	5	95
15.8	1.0	5	95
15.9	1.0	95	5
30.0	1.0	95	5

Table 3

Composition (A) and physicochemical properties (B) of simulated mouse-rat ISF (SMR-ISF) and simulated human-monkey ISF (SHM-ISF).

(A)	Blank ISF	SMR-ISF	SHM-ISF
NaCl (mM)	101.6	101.6	101.6
KCl (mM)	10.0	10.0	10.0
MgCl ₂ (mM)	0.9	0.9	0.9
Na ₂ HPO ₄ (mM)	17.6	17.6	17.6
NaH ₂ PO ₄ (mM)	2.2	2.2	2.2
BSA (g/L)	–	17.5	30.0

(B)	Blank ISF	SMR-ISF	SHM-ISF
pH	7.4 ± 0.1	7.4 ± 0.1	7.4 ± 0.1
Buffer Capacity (µmol/(mL*ΔpH))	10.5 ± 0.1	11.3 ± 0.2	13.1 ± 0.3
Osmolality (mOsm/kg)	255 ± 1	281 ± 5	290 ± 2
Colloid Osmotic Pressure (mmHg)	0	6.8 ± 0.1	14.2 ± 0.1
Surface Tension (mN/m)	69.8 ± 0.1	59.4 ± 0.5	58.3 ± 0.4

SISF, which has no colloid osmotic pressure due to the absence of large biomolecules, the colloid osmotic pressure increased on average to 6.8 (SMR-ISF) and 14.2 (SHM-ISF) mmHg. In contrast, the surface tension decreased, which is also consistent with the previously reported physicochemical properties of albumin solutions (Thi-Yen Le et al., 2022).

4.2. Stability of the simulated interstitial fluids

The SISFs containing 0.05 % sodium azide proved to be stable in terms of pH, buffer capacity, osmolality, and surface tension at storage (5 °C) and testing (34 °C, 75 rpm) conditions, as can be seen from Table 4. Moreover, visual inspection detected no signs of instability.

4.3. *In vitro* diffusion testing

The mean diffusion profiles obtained from the *in vitro* diffusion experiments are presented in Fig. 3.

In both the MR- and the HM model the highest liraglutide diffusion rates were observed when the respective SISF at the apical side was combined with SPlasma without albumin (Blank SPlasma) at the basolateral side. By contrast, the combination of SISF and SPlasma for the same species (i.e., SMR-ISF:SMR-Plasma and SHM-ISF:SHM-Plasma) with otherwise identical experimental design, resulted in lower diffusion rates with a 1.3- and 1.7-fold lower total amount of liraglutide that reached the basolateral side within the test duration of 8 h in the MR- and HM model, respectively. This phenomenon can be explained by the fact that not only liraglutide but also albumin was able to diffuse through the hydrogel layer and the membrane in the experimental setup used, as shown by the HPLC analysis of the samples from the basolateral compartment. Although not originally intended to detect or quantify albumin in the simulated plasma medium, a previously absent albumin elution peak appeared in the Blank SPlasma chromatograms as the

Table 4

Stability data for simulated mouse-rat ISF (SMR-ISF) and simulated human-monkey ISF (SHM-ISF) at storage (5 °C) and testing (34 °C, 75 rpm) conditions over the course of 8 days.

	Sampling (days)	SMR-ISF		SHM-ISF	
		Storage	Testing	Storage	Testing
pH	0	7.4 ± 0.0	7.4 ± 0.0	7.4 ± 0.0	7.4 ± 0.0
	1	7.4 ± 0.0	7.4 ± 0.0	7.4 ± 0.0	7.4 ± 0.0
	3	7.4 ± 0.0	7.4 ± 0.0	7.4 ± 0.0	7.4 ± 0.0
	8	7.4 ± 0.0	7.4 ± 0.0	7.4 ± 0.0	7.4 ± 0.0
Buffer Capacity (μmol/ (mL·ΔpH))	0	11.0 ± 0.0	11.0 ± 0.1	12.6 ± 0.4	12.6 ± 0.4
	1	11.0 ± 0.1	11.0 ± 0.3	12.1 ± 0.2	12.0 ± 0.0
	3	10.6 ± 0.3	11.0 ± 0.2	12.1 ± 0.2	12.0 ± 0.1
	8	11.5 ± 0.1	11.5 ± 0.3	12.5 ± 0.3	13.5 ± 0.5
Osmolality (mOsm/kg)	0	281 ± 5	281 ± 5	281 ± 5	290 ± 2
	1	282 ± 3	290 ± 3	276 ± 2	287 ± 3
	3	282 ± 1	291 ± 2	280 ± 1	292 ± 1
	8	284 ± 1	295 ± 1	285 ± 3	296 ± 1
Surface Tension (mN/m)	0	62.2 ± 0.6	62.2 ± 0.6	56.1 ± 0.9	56.1 ± 0.9
	1	56.1 ± 1.0	60.8 ± 1.0	56.9 ± 1.6	57.2 ± 1.0
	3	57.3 ± 1.2	60.1 ± 0.7	58.4 ± 0.7	58.2 ± 0.7
	8	57.4 ± 0.5	57.2 ± 0.7	57.7 ± 0.9	58.3 ± 1.0

diffusion experiment progressed. This peak increased steadily with time, indicating that the albumin concentration in the basolateral compartment was increasing. As the purpose of the HPLC analysis was to determine the concentration of liraglutide, no calibration curve was included for the quantification of albumin, so the albumin content in each sample could not be measured quantitatively. However, when samples from both the basolateral (Blank SPlasma) and apical (SMR-ISF or SHM-ISF) compartments, were analyzed at the last sampling time (8

h), a similarly large signal was detected in both chromatograms, indicating that albumin equilibrium had been achieved between the two compartments.

The fact that albumin can cross the diffusion barrier in the *in vitro* model used provides an explanation for the increased diffusion rate of liraglutide in experiments using Blank SPlasma in the basolateral compartment. As liraglutide binds to albumin, not only unbound drug but also drug bound to albumin can pass the diffusion barrier, so that higher diffusion rates and greater amounts of liraglutide were observed in the basolateral compartment during the period studied when it did not contain albumin at the start of the test.

In order to better understand the effect of albumin on the diffusion of liraglutide, the molar concentrations of albumin and liraglutide in the different compartments (apical compartment, matrix and basolateral compartment) were calculated for each of the experiments performed (Table 5). For this purpose, first, the molar concentration of albumin was calculated in the following volumes: 100 μL SISF (17.5 g/L and 30 g/L albumin for the SMR- and SHM-ISF, respectively), 1.5 mL SPlasma (25 g/L and 60 g/L for the SMR- and SHM-plasma, respectively) and 1 mL of a 60 μM albumin solution used for the preparation of the matrix. Then, the molar ratio between albumin and liraglutide in the different compartments was calculated considering the test volume of 50 μL of a 6 mg/mL liraglutide formulation (i.e. $7.99 \cdot 10^{-2}$ μmol) and assuming that the liraglutide dose would exclusively be present in the compartment of interest at that moment.

As shown in Table 5, the molar concentration of liraglutide in the apical compartment was 3.03- and 1.76 times higher than that of albumin for the SMR- and SHM-ISF, respectively. Therefore, even if liraglutide binds 95 % to albumin, an excess of free liraglutide will be present in both SISFs. At this point, it is important to note that previous studies have indicated that liraglutide tends to form heptamers in

Table 5

Albumin content in the different compartments of the *in vitro* model and molar ratio between albumin and liraglutide, assuming that the complete liraglutide dose would be present in the respective compartment.

	SMR-ISF	SHM-ISF	SMR-Plasma	SHM-Plasma	Matrix
Albumin (μmol)	$2.63 \cdot 10^{-2}$	$4.52 \cdot 10^{-2}$	0.56	1.35	$6.00 \cdot 10^{-2}$
Molar ratio	1:3.03	1:1.76	1:0.14	1:0.06	1:1.33
Albumin: Liraglutide ¹					

¹ For the molar ratio, a dose of $7.99 \cdot 10^{-2}$ μmol of liraglutide was considered.

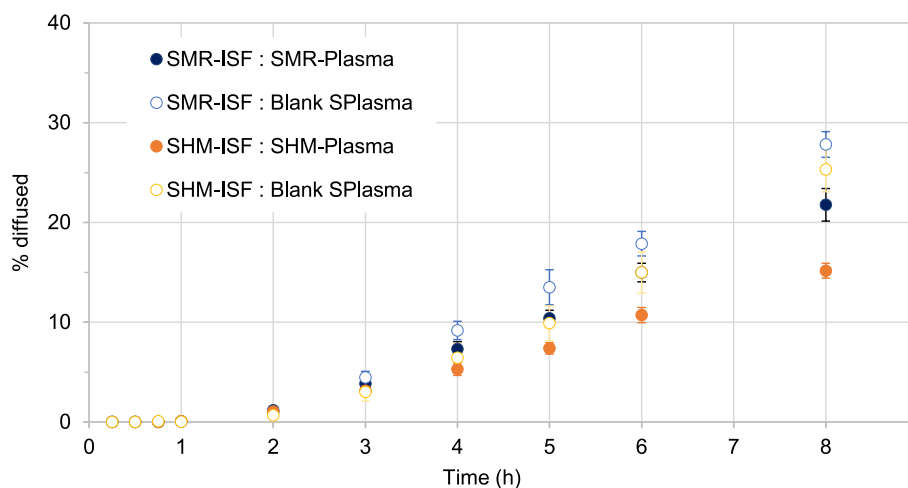


Fig. 3. *In vitro* liraglutide diffusion profiles obtained when mimicking ISF composition of different species (mouse-rat in blue and human-monkey in orange) in the modified artificial subcutaneous tissue assay (mean of $n = 5 \pm$ SD.) The lighter colors for both models indicate the experiments where no albumin was added to the simulated plasma (Blank SPlasma). (For interpretation of the references to color in this figure legend, the reader is referred to the web version of this article.)

solution (Frederiksen et al., 2015). *In vivo*, this might have a significant impact on the diffusion rate. This phenomenon might also affect the diffusion rate observed in the present set of *in vitro* experiments. However, since with a molecular weight of 7 times $\sim 3,8$ kDa (Frederiksen et al., 2015), these heptamers are still significantly smaller than an albumin molecule (~ 66.5 kDa) and in the present experimental setup albumin can diffuse through the membrane and the matrix separating the apical and basolateral compartments, it is unlikely that heptamer formation precludes diffusion into the basolateral compartment. It would certainly be interesting to know, whether the diffusion rate of individual liraglutide molecules differs from that of heptamers. The primary aim of this first study, however, was a very first evaluation of the influence of the basic composition of SISFs on the diffusion of a fixed dose of liraglutide from the simulated interstitial space into simulated plasma.

The *in vitro* diffusion model used in the present study is based on a subcutaneous permeation model recently developed by Schöner et al. which focuses on the simulation of the extracellular matrix but not on the simulation of the ISF. Accordingly, in Schöner's experiments, which aimed to investigate the permeation of insulins from the SC tissue into the bloodstream under biorelevant conditions, no SISF was used on the apical side (Schöner et al., 2024). In the current model, the recently developed biomatrix consisting of physiologically relevant mass ratios of collagen and hyaluronic acid (Aukland and Reed, 1993; Wiig and Swartz, 2012) was maintained and overlaid with 100 μ L of a SISF into which 50 μ L of the liraglutide solution under investigation was "injected", so that the influence of physiologically relevant albumin concentrations on the diffusion of liraglutide from the interstitial space into the plasma could be studied. After interaction with the SISF, the albumin-bound and unbound liraglutide must diffuse through the uniformly polymerized matrix of 2 mg/ml collagen and 0.1 % hyaluronic acid. In addition to collagen and hyaluronic acid, albumin is part of the matrix composition. The latter was added to prevent the drugs tested from adhering to the plastic material of the Transwell plate and to enable the analysis of albumin-binding drugs in the future. In these first experiments with liraglutide, the composition of the matrix was not changed. It should be noted, however, that the albumin concentration does not correspond to that of the SISFs used and is higher than that of either SISF, so diffusion is most likely not only controlled by the composition of the SISF, but also by the composition and structure of the matrix. As the latter was the same in all experiments, it seemed possible to make an

initial cautious distinction regarding the SISF composition based on the results obtained. Nevertheless, to get a better idea of how much the SISF compositions as such would affect diffusion, a second set of diffusion experiments was performed with identical test conditions but omitting the use of the matrix in the Transwell setup. The results obtained are shown in Fig. 4.

As expected, diffusion was much faster in the absence of the matrix and equilibrium was reached in all experiments within 8 h. Overall, the diffusion experiments without the matrix confirm the trend observed in the results with matrix, i.e. in experiments where blank SPlasma was used on the basolateral side, higher diffusion rates were observed and in the SHM-SIF:SHM plasma model the lowest liraglutide concentration was measured on the basolateral side throughout the experiment. In both test series, i.e., with and without matrix, it was possible to clearly differentiate between the MR and the HM model in the experiments with SISF on the apical and SPlasma on the basolateral side.

When discussing the permeability of the matrix used and the membrane underneath, it should be mentioned that both allow bidirectional diffusion of liraglutide, albumin and albumin-bound liraglutide, a phenomenon that by no means corresponds to *in vivo* conditions and can lead to an equilibrium over the duration of the experiment. This will need to be better adapted to the real physiological conditions in future work. In addition, consideration should be given to how the physiological conditions can be scaled down in a meaningful way in relation to the volumes and matrix dimensions used. In the present series of experiments, SPlasma and Blank SPlasma were used on the basolateral side. The lower diffusion rates observed in the experiments with SPlasma and the overall smaller amount of liraglutide in the basolateral compartment at the end of these experiment is certainly a result of the fact that the albumin concentration in SPlasma is significantly higher than in SISF, regardless of the species simulated, which leads to increased diffusion of albumin from the basolateral compartment into the apical compartment due to the permeability of both membrane and matrix. From the moment liraglutide diffuses into SPlasma, it can be bound to albumin and thus possibly transported back again. It would be too speculative to discuss further which of the complex bidirectional diffusion processes dominates here, but the results obtained clearly indicate the existence of competing processes. *In vivo*, the higher plasma albumin concentration compared to ISF does not lead to albumin diffusion into tissues, so an optimal *in vitro* model should not allow this diffusion pathway. Furthermore, once liraglutide appears in plasma, it is

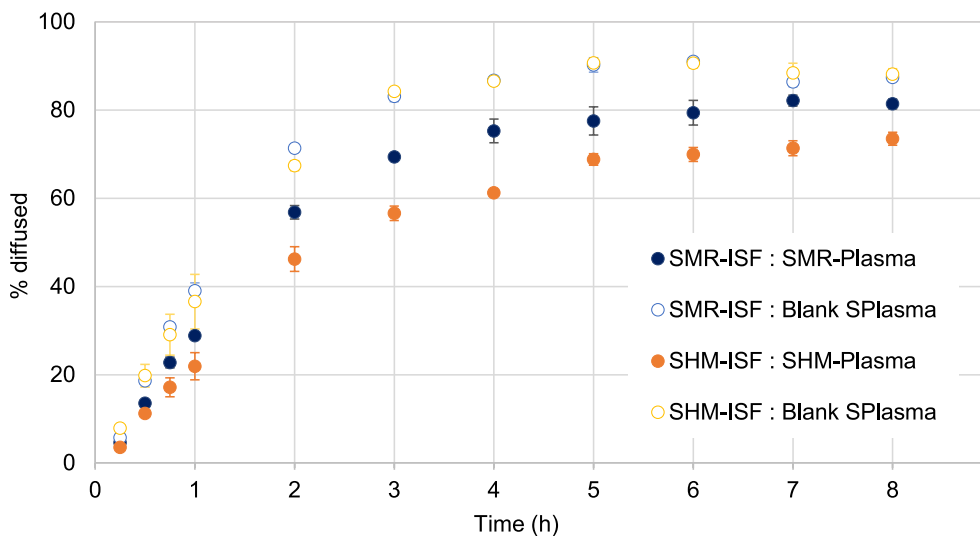


Fig. 4. *In vitro* liraglutide diffusion profiles obtained when mimicking ISF composition of different species (mouse-rat in blue and human-monkey in orange) in the modified artificial subcutaneous tissue assay (mean of $n = 3 \pm$ SD) without the simulated extracellular matrix. The lighter color for both models indicate the experiments where no albumin was added to the simulated plasma (Blank SPlasma). (For interpretation of the references to color in this figure legend, the reader is referred to the web version of this article.)

immediately distributed throughout the plasma volume, regardless of whether it is bound to plasma albumin, free or forming heptamers. Accordingly, sink conditions must also be considered when designing an *in vitro* model. Currently, the *in vitro* model is not considered to represent adequate sink conditions. Due to the expected unidirectional drug transport, at least in the early phases of the experiment, such conditions are more likely to exist, if any, in the *in vitro* model using Blank SPLasma in the basolateral compartment. Overall, however, it must be concluded that the *in vitro* diffusion model is still far from being sufficiently differentiated to be able to estimate the influences of the composition of SISFs of different species on the bioavailability of SC-administered drugs. Future activities will therefore have to focus on the further development of this model, but also on the establishment of simpler models that can be used to obtain a better mechanistic understanding of the individual influencing factors in the very complex processes of SC drug absorption, to which, in addition to the diffusion processes discussed, the possibility of lymphatic absorption of albumin-bound active substances, a phenomenon known as albumin hitchhiking (Abdallah et al., 2020), can contribute.

Given that several alternative *in vitro* models have been developed in the recent past, such as the SCISSOR (Kinnunen et al., 2015), it may be questioned whether it is appropriate to continue with the test concept used. However, it should be noted that the establishment of the matrix, which mimics the main components of the extracellular matrix and whose albumin content can be easily adapted to the species to be simulated in future experiments (Schöner et al., 2024), and the SISFs established in the present study for the preclinical species mice and rats, as well as for humans and monkeys, are two major steps towards a biorelevant *in vitro* model, which now need to be specifically combined and further developed. Compared to other test methods described in the literature, the Transwell-based *in vitro* model, which is tubeless and does not require a pump, carries a lower overall risk of adsorption effects and mechanical stress on the tested formulations, especially in the case of testing biologicals. If the shortcomings discussed above are adequately addressed, it will provide an interesting biorelevant screening tool that allows for high throughput, provides results that are not subject to the high variability of *in vivo* studies, and can be used in both formulation development and quality control.

5. Conclusion

Based on data from a previous characterization study of subcutaneous ISFs, the present study developed SISFs for the preclinical species mice and rats, as well as for humans and monkeys. The focus was on the albumin content and the physicochemical properties pH, buffer capacity, osmolality, colloid osmotic pressure, and surface tension. It was observed that the different albumin concentrations in the species-specific media influenced the physicochemical properties of the media and that the higher albumin content in SHM-ISF was reflected in a higher buffer capacity and a lower surface tension, correlating with the biological ISF reference samples. In initial stability studies, the physical stability of the developed SISFs was shown to be suitable for storage at refrigerator temperature and for conducting *in vitro* release studies at 34 °C for 8 days each. The newly developed media were used in initial *in vitro* diffusion studies with a commercial injectable preparation of liraglutide, a drug that binds to ≥ 95 % of albumin. Although the *in vitro* model used for this purpose still needs to be significantly modified, these two new media will undoubtedly help to gain a better understanding of the *in vivo* performance of subcutaneously injected formulations and will make an important contribution to better understanding how results obtained in preclinical species can be extrapolated to humans and, more importantly, to avoiding unnecessary animal testing.

CRedit authorship contribution statement

Iria Torres-Terán: Writing – original draft, Methodology,

Investigation, Conceptualization. Márta Venczel: Writing – review & editing, Supervision, Project administration, Methodology, Funding acquisition, Conceptualization. Sandra Klein: Writing – review & editing, Supervision.

Declaration of competing interest

The authors declare that they have no known competing financial interests or personal relationships that could have appeared to influence the work reported in this paper.

Data availability

Data will be made available on request.

Acknowledgments

The research described in this paper was sponsored by a Ph.D. grant from Sanofi. Authors would like to thank Daniel Wagner for his support. Moreover, the authors would like to thank Andrea Weidner for her support with the HPLC analysis.

References

- Abdallah, M., Müllertz, O.O., Styles, I.K., Mörsdorf, A., Quinn, J.F., Whittaker, M.R., Trevasik, N.L., 2020. Lymphatic targeting by albumin-hitchhiking: Applications and optimisation. *J. Control. Release* 327, 117–128. <https://doi.org/10.1016/j.jconrel.2020.07.046>.
- Aukland, K., Reed, R.K., 1993. Interstitial-lymphatic mechanisms in the control of extracellular fluid volume. *Physiol. Rev.* 73 (1), 1–78. <https://doi.org/10.1152/physrev.1993.73.1.1>.
- Bender, C., Eichling, S., Franzen, L., Herzog, V., Ickenstein, L.M., Jere, D., Nonis, L., Schwach, G., Stoll, P., Venczel, M., Zenk, S., 2022. Evaluation of *in vitro* tools to predict the *in vivo* absorption of biopharmaceuticals following subcutaneous administration. *J. Pharm. Sci.* 111 (9), 2514–2524. <https://doi.org/10.1016/j.xphs.2022.04.005>.
- Bock, F., Lin, E., Larsen, C., Jensen, H., Huus, K., Larsen, S.W., Østergaard, J., 2020. Towards *in vitro* *in vivo* correlation for modified release subcutaneously administered insulins. *Eur. J. Pharm. Sci.* 145, 1–10. <https://doi.org/10.1016/j.ejps.2020.105239>.
- Cai, X., Luan, Y., Jiang, Y., Song, A., Shao, W., Li, Z., Zhao, Z., 2012. Huperzine A-phospholipid complex-loaded biodegradable thermosensitive polymer gel for controlled drug release. *Int. J. Pharm.* 433 (1–2), 102–111. <https://doi.org/10.1016/j.ijpharm.2012.05.009>.
- Chu, D.F., Fu, X.Q., Liu, W.H., Liu, K., Li, Y.X., 2006. Pharmacokinetics and *in vitro* and *in vivo* correlation of huperzine A loaded poly(lactic-co-glycolic acid) microspheres in dogs. *Int. J. Pharm.* 325 (1–2), 116–123. <https://doi.org/10.1016/j.ijpharm.2006.06.032>.
- Collins, D.S., Sánchez-Félix, M., Badkar, A.V., Mrsny, R., 2020. Accelerating the development of novel technologies and tools for the subcutaneous delivery of biotherapeutics. *J. Control. Release* 321, 475–482. <https://doi.org/10.1016/j.jconrel.2020.02.036>.
- D'Arcy, D.M., Wacker, M.G., Klein, S., Shah, V., Burke, M.D., Hunter, G., Xu, H., 2022. *In-vitro* product performance of parenteral drug products: view of the USP expert panel. *Dissolution Technol.* 29, 204–218. <https://doi.org/10.14227/DT290422P204>.
- D'Souza, S., Faraj, J.A., Giovagnoli, S., DeLuca, P.P., 2014. *In vitro*–*in vivo* correlation from lactide-co-glycolide polymeric dosage forms. *Prog. Biomater.* 3 (2–4), 131–142. <https://doi.org/10.1007/s40204-014-0029-4>.
- Del Curto, M.D., Chicco, D., D'Antonio, M., Ciolli, V., Dannan, H., D'Urso, S., Neuteboom, B., Pompili, S., Schiesaro, S., Esposito, P., 2003. Lipid microparticles as sustained release system for a GnRH antagonist (Antide). *J. Control. Release* 89 (2), 297–310. [https://doi.org/10.1016/S0168-3659\(03\)00120-2](https://doi.org/10.1016/S0168-3659(03)00120-2).
- Díaz de León-Ortega, R., D'Arcy, D.M., Lamprou, D.A., Xue, W.F., Fotaki, N., 2021. *In vitro* *in vivo* relations for the parenteral liposomal formulation of Amphotericin B: A biorelevant and clinically relevant approach. *Eur. J. Pharm. Biopharm.* 159, 188–197. <https://doi.org/10.1016/j.ejpb.2020.07.025>.
- Doty, A.C., Weinstein, D.G., Hirota, K., Olsen, K.F., Ackermann, R., Wang, Y., Choi, S., Schwendeman, S.P., 2017. Mechanisms of *in vivo* release of triamcinolone acetonide from PLGA microspheres. *J. Control. Release* 256, 19–25. <https://doi.org/10.1016/j.jconrel.2017.03.031>.
- Dubbelboer, I.R., Sjögren, E., 2022. Overview of authorized drug products for subcutaneous administration: Pharmaceutical, therapeutic, and physicochemical properties. *Eur. J. Pharm. Sci.* 173, 106181. <https://doi.org/10.1016/j.ejps.2022.106181>.
- Frederiksen, T.M., Sønderby, P., Ryberg, L.A., Harris, P., Bukrinski, J.T., Scharff-Poulsen, A.M., Elf-Lind, M.N., Peters, G.H., 2015. Oligomerization of a Glucagon-like Peptide 1 Analog: Bridging Experiment and Simulations. *Biophys. J.* 109 (6), 1202–1213. <https://doi.org/10.1016/j.bpj.2015.07.051>.

- Gao, G.F., Thurn, M., Wendt, B., Parnham, M.J., Wacker, M.G., 2020. A sensitive in vitro performance assay reveals the in vivo drug release mechanisms of long-acting medroxyprogesterone acetate microparticles. *Int. J. Pharm.* 586, 119540. <https://doi.org/10.1016/j.ijpharm.2020.119540>.
- Gao, G.F., Ashtikar, M., Kojima, R., Yoshida, T., Kaihara, M., Tajiri, T., Shانهsazzadeh, S., Modh, H., Wacker, M.G., 2021. Predicting drug release and degradation kinetics of long-acting microsphere formulations of tacrolimus for subcutaneous injection. *J. Control. Release* 329, 372–384. <https://doi.org/10.1016/j.jconrel.2020.11.055>.
- Gao, P., Xu, H., Ding, P., Gao, Q., Sun, J., Chen, D., 2007. Controlled release of huperzine A from biodegradable microspheres: In vitro and in vivo studies. *Int. J. Pharm.* 330 (1–2), 1–5. <https://doi.org/10.1016/j.ijpharm.2006.08.030>.
- Iyer, S.S., Barr, W.H., Dance, M.E., Coleman, P.R., Karnes, H.T., 2007. A “biorelevant” system to investigate in vitro drug released from a naltrexone implant. *Int. J. Pharm.* 340 (1–2), 104–118. <https://doi.org/10.1016/j.ijpharm.2007.03.032>.
- Jablonka, L., Ashtikar, M., Gao, G., Jung, F., Thurn, M., Preuß, A., Scheglmann, D., Albrecht, V., Röder, B., Wacker, M.G., 2019. Advanced in silico modeling explains pharmacokinetics and biodistribution of temoporfin nanocrystals in humans. *J. Control. Release* 308, 57–70. <https://doi.org/10.1016/j.jconrel.2019.06.029>.
- Kinnunen, H.M., Sharma, V., Contreras-Rojas, L.R., Yu, Y., Alleman, C., Sreedhara, A., Fischer, S., Khawli, L., Yohe, S.T., Bumbaca, D., Patapoff, T.W., Daugherty, A.L., Mrsny, R.J., 2015. A novel in vitro method to model the fate of subcutaneously administered biopharmaceuticals and associated formulation components. *J. Control. Release* 214, 94–102. <https://doi.org/10.1016/j.jconrel.2015.07.016>.
- Klein, S., 2010. The use of biorelevant dissolution media to forecast the in vivo performance of a drug. *AAPS J.* 12, 397–406. <https://doi.org/10.1208/s12248-010-9203-3>.
- Lee, D.S., Kang, D.W., Choi, G.W., Choi, H.G., Cho, H.Y., 2020. Development of level a in vitro–vivo correlation for electrosprayed microspheres containing leuprolide: Physicochemical, pharmacokinetic, and pharmacodynamic evaluation. *Pharmaceutics* 12 (1), 36. <https://doi.org/10.3390/pharmaceutics12010036>.
- Li, X., Zhao, Z., Li, L., Zhou, T., Lu, W., 2015. Pharmacokinetics, in vitro and in vivo correlation, and efficacy of exenatide microspheres in diabetic rats. *Drug Deliv.* 22 (1), 86–93. <https://doi.org/10.3109/10717544.2013.871760>.
- Lou, H., Hageman, M.J., 2023. Development of Drug Release Model for Suspensions in ESCAR (Emulator of SubCutaneous Absorption and Release). *AAPS J.* 25 (3), 29. <https://doi.org/10.1208/s12248-023-00799-1>.
- Negrín, C.M., Delgado, A., Llabrés, M., Évora, C., 2004. Methadone implants for methadone maintenance treatment. In vitro and in vivo animal studies. *J. Control. Release* 95 (3), 413–421. <https://doi.org/10.1016/j.jconrel.2003.12.008>.
- Nippe, S., Preuß, C., General, S., 2013. Evaluation of the in vitro release and pharmacokinetics of parenteral injectable formulations for steroids. *Eur. J. Pharm. Biopharm.* 83 (2), 253–265. <https://doi.org/10.1016/j.ejpb.2012.09.006>.
- Rawat, A., Bhardwaj, U., Burgess, D.J., 2012. Comparison of in vitro-in vivo release of Risperdal® Consta® microspheres. *Int. J. Pharm.* 434 (1–2), 115–121. <https://doi.org/10.1016/j.ijpharm.2012.05.006>.
- Rees, 2011. pH Buffer Design: AQIX RS-I. doi: 10.13140/RG.2.1.2902.6161.
- Rees, D., 2011. Unique Design of RS-I. doi: 10.13140/RG.2.1.1198.6804.
- Sánchez-Félix, M., Burke, M., Chen, H.H., Patterson, C., Mittal, S., 2020. Predicting bioavailability of monoclonal antibodies after subcutaneous administration: Open innovation challenge. *Adv. Drug Deliv. Rev.* 167, 66–77. <https://doi.org/10.1016/j.addr.2020.05.009>.
- Schöner, T.A., Vogel, V., Venczel, M., Knoth, K., Kamm, W., Paehler, T., Louit, G., Torres-Terán, I., Munding, P., Marker, A., Loos, P., Hittinger, M., Lehr, C.-M., 2024. Biorelevant subcutaneous in vitro test predicts the release of human and fast acting insulin formulations. *Int. J. Pharm.* 655, 123995. <https://doi.org/10.1016/j.ijpharm.2024.123995>.
- Solano, A.G.R., De Fátima Pereira, A., Pinto, F.C.H., Ferreira, L.G.R., De Oliveira Barbosa, L.A., Fialho, S.L., De Oliveira Patricio, P.S., Da Silva Cunha, A., Da Silva, G. R., Pianetti, G.A., 2013. Development and evaluation of sustained-release etoposide-loaded poly(ϵ -caprolactone) implants. *AAPS PharmSciTech* 14 (2), 890–900. <https://doi.org/10.1208/s12249-013-9977-6>.
- Summary of Product Characteristics: Liraglutide, 2022. Available at https://www.ema.europa.eu/en/documents/product-information/victoza-epar-product-information_en.pdf (Accessed on: 10 Jan 2022).
- Sun, Y., Peng, Y., Aksornkoae, N., Johnson, J.R., Boring, J.G., Scruggs, D., Cooper, R.C., Laizure, S.C., Shukla, A.J., 2002. Controlled release of oxytetracycline in sheep. *J. Control. Release* 85 (1–3), 125–134. [https://doi.org/10.1016/S0168-3659\(02\)00286-9](https://doi.org/10.1016/S0168-3659(02)00286-9).
- Sun, Y., Wang, J.C., Zhang, X., Zhang, Z.J., Zheng, Y., Chen, D.W., Zhang, Q., 2008. Synchronic release of two hormonal contraceptives for about one month from the PLGA microspheres: In vitro and in vivo studies. *J. Control. Release* 129 (3), 192–199. <https://doi.org/10.1016/j.jconrel.2008.04.022>.
- Thi-Yen Le, T., Hussain, S., Tsay, R.Y., Noskov, B.A., Akentiev, A., Lin, S.Y., 2022. On the equilibrium surface tension of aqueous protein solutions – Bovine serum albumin. *J. Mol. Liq.* 347, 118305. <https://doi.org/10.1016/j.molliq.2021.118305>.
- Torres-Terán, I., Venczel, M., Klein, S., 2021. Prediction of subcutaneous drug absorption - do we have reliable data to design a simulated interstitial fluid? *Int. J. Pharm.* 610, 1–16. <https://doi.org/10.1016/j.ijpharm.2021.121257>.
- Torres-Terán, I., Venczel, M., Stieler, T., Parisi, L., Kloss, A., Klein, S., 2023. Prediction of subcutaneous drug absorption – Characterization of subcutaneous interstitial fluids as a basis for developing biorelevant in vitro models. *Int. J. Pharm.* 638, 122906. <https://doi.org/10.1016/j.ijpharm.2023.122906>.
- Viola, M., Sequeira, J., Seica, R., Veiga, F., Serra, J., Santos, A.C., Ribeiro, A.J., 2018. Subcutaneous delivery of monoclonal antibodies: How do we get there? *J. Control. Release* 286, 301–314. <https://doi.org/10.1016/j.jconrel.2018.08.001>.
- Vlugt-Wensink, K.D.F., De Vruhe, R., Gresnigt, M.G., Hoogerbrugge, C.M., Van Buul-Offers, S.C., De Leede, L.G.J., Sterkman, L.G.W., Crommelin, D.J.A., Hennink, W.E., Verrijck, R., 2007. Preclinical and clinical in vitro in vivo correlation of an hGH dextran microsphere formulation. *Pharm. Res.* 24 (12), 2239–2248. <https://doi.org/10.1007/s11095-007-9433-y>.
- Wallenwein, C.M., Nova, M.V., Janas, C., Jablonka, L., Gao, G.F., Thurn, M., Albrecht, V., Wiehe, A., Wacker, M.G., 2019. A dialysis-based in vitro drug release assay to study dynamics of the drug-protein transfer of temoporfin liposomes. *Eur. J. Pharm. Biopharm.* 143, 44–50. <https://doi.org/10.1016/j.ejpb.2019.08.010>.
- Wiig, H., Swartz, M.A., 2012. Interstitial fluid and lymph formation and transport: Physiological regulation and roles in inflammation and cancer. *Physiol. Rev.* 92 (3), 1005–1060. <https://doi.org/10.1152/physrev.00037.2011>.
- Xuan, J., Lin, Y., Huang, J., Yuan, F., Li, X., Lu, Y., Zhang, H., Liu, J., Sun, Z., Zou, H., Chen, Y., Gao, J., Zhong, Y., 2013. Exenatide-loaded PLGA microspheres with improved glyceimic control: In vitro bioactivity and in vivo pharmacokinetic profiles after subcutaneous administration to SD rats. *Peptides* 46, 172–179. <https://doi.org/10.1016/j.peptides.2013.06.005>.
- Zheng, Y., Tesar, D.B., Benincosa, L., Birnböck, H., Boswell, C.A., Bumbaca, D., Cowan, K. J., Danilenko, D.M., Daugherty, A.L., Fielder, P.J., Grimm, H.P., Joshi, A., Justies, N., Kolaitis, G., Lewin-Koh, N., Li, J., McVay, S., O'Mahony, J., Otteneder, M., Pantze, M., Putnam, W.S., Qiu, Z.J., Ruppel, J., Singer, T., Stauch, O., Theil, F.P., Visich, J., Yang, J., Ying, Y., Khawli, L.A., Richter, W.F., 2012. Minipig as a potential translatable model for monoclonal antibody pharmacokinetics after intravenous and subcutaneous administration. *MAbs* 4 (2), 243–255. <https://doi.org/10.4161/mabs.4.2.19387>.